

## Research Paper

# A Novel Method to Radiolabel Gastric Retentive Formulations for Gamma Scintigraphy Assessment

Matthew D. Burke,<sup>1,4</sup> J. Scott Staton,<sup>2</sup> Ann W. Vickers,<sup>3</sup> Erin E. Peters,<sup>3</sup> and Mark D. Coffin<sup>1</sup>

Received August 17, 2006; accepted November 6, 2006; published online February 15, 2007

**Purpose.** To develop a robust radiolabeling technique to enable evaluation of difficult to radiolabel gastric retentive formulations using gamma scintigraphy. The use of a successful radiolabel will allow accurate assessment of the gastric residence time of the formulations.

**Materials and Methods.** The retention of two radionuclides, indium (<sup>111</sup>In) and samarium (<sup>153</sup>Sm), with and without further processing to improve radiolabel performance were evaluated in simulated gastric pH *in vitro*. The most successful formulation from the *in vitro* screening was further evaluated in preclinical and clinical studies.

**Results.** *In vitro* evaluation revealed significant radionuclide leakage at pH 1.5 for most radiolabeling attempts. Radionuclide leakage at pH 4.5 was less pronounced. The most successful radiolabel was formulated by adsorbing indium chloride onto activated charcoal, followed by entrapment in a cellulose acetate polymer melt. This provided the best radiolabel retention under both pH conditions *in vitro*. The radiolabel also proved to be successful during preclinical and clinical evaluations, allowing evaluation of gastric retention performance as well as complete gastrointestinal transit.

**Conclusion.** A simple, yet robust radiolabel was developed for gastric retentive formulations to be evaluated pre-clinically or in a clinical setting by entrapping the radionuclide in an insoluble polymer through a simple polymer melt process.

**KEY WORDS:** gamma scintigraphy; gastric retentive formulations; gastroretention; indium chloride; radiolabel.

## INTRODUCTION

Gastric retentive formulations (GRFs) have been pursued by both academia and industry for an extensive period of time, due to the clear benefits of such a formulation for drug substances with narrow window of absorption, local treatment or other challenging pharmacokinetic/pharmacodynamic situations. Gastric retentive strategies can be divided into five basic categories: floating, high density, bioadhesive, large size and gastric motility agents. A significant number of GRFs fall into the category of gastric retention based on a large size (1–4). However, the size required for gastric retention is not clearly known. Based on

endoscopic data from ingestion of large foreign objects and gastric bezoars, a large, fairly rigid object must be of a size larger than 5 cm in length by 2 cm in diameter to be retained for an extensive period of time in the stomach (5–7). Endoscopic guidance recommends that if the foreign object does not pose an immediate health risk and if it is smaller than the previously stated size, a surgical intervention is not required and the object should pass out of the stomach spontaneously (5,6). Although, this information is far from a controlled evaluation of the sizes and mechanical strength required to identify an ideal GRF, it does provide guidance on the size and the volumetric expansion of the formulation required for gastric retention. To obtain this size (5 cm length × 2 cm diameter) and be still able to be dosed in a pharmaceutically acceptable format (e.g. 000 capsule) the amount of volumetric swelling needs to be on the order of 15 times the original size. This is quite a formidable task but can be achieved with the proper formulation.

The ultimate success of a GRF is based on the achievement of an acceptable pharmacokinetic profile and oral bioavailability of the drug substance; however, alternative approaches can first be applied to determine if a formulation is truly retained in the stomach. Ideally, a non-invasive approach which does not alter the physical properties of the GRF is preferred. Magnetic resonance imaging is gaining popularity in this area (8). Another option is the use of a swallowable camera in the form of a capsule (9); video

<sup>1</sup>Product Development, Pharmaceutical Development, Glaxo SmithKline, 5 Moore Drive, Research Triangle Park, NC 27709, USA.

<sup>2</sup>Strategic Technologies, Pharmaceutical Development, Glaxo SmithKline, 5 Moore Drive, Research Triangle Park, NC 27709, USA.

<sup>3</sup>Biopharmaceutics, Pharmaceutical Development, GlaxoSmith Kline, 5 Moore Drive, Research Triangle Park, NC 27709, USA.

<sup>4</sup>To whom correspondence should be addressed. (e-mail: matthew.d.burke@gsk.com)

**ABBREVIATIONS:** GRF, gastric retentive formulation; In, indium; Sm, samarium; Tc, technetium; eV, electron volts; BMI, body mass index; ROI, region of interest; PEIC, polymer encapsulated <sup>111</sup>indium chloride; GI, gastrointestinal.

resolution for the swallowable camera is exceptional; however, battery life is limited and controlling the orientation and gastrointestinal transit of the camera is not possible at this time. Another emerging technology is Magnetic Marker Monitoring (10). In this approach, the dosage form is marked as a permanent magnetic dipole by the incorporation of small amounts of ferromagnetic material. Gamma scintigraphy has been used extensively for tracking the location of dosage forms *in vivo* and is often referred to as the “gold standard” for transit studies (11). To perform gamma scintigraphy, a small amount of a radioactivity is incorporated into the dosage form which emits gamma rays that can be detected with a gamma camera to determine the location of the dosage form in the body. The limitations of such an approach are mainly cost and appropriate use of a gamma camera. The ideal photon energy for radionuclides is between 100–200 keV; below this range resolution decreases due to tissue scatter and above this range sensitivity decreases. Another important aspect of the radionuclide is the half-life, which impacts the length of time that one can image a radiolabeled formulation. Samarium, indium and technetium are three common radionuclides used in gamma scintigraphy studies with good photon energy and a suitable half-life. The half-life of  $^{153}\text{Sm}$  is 46.2 h and the photon energy is 103 keV,  $^{111}\text{In}$  half-life is 2.8 days and the photon energy is 247 keV and  $^{99\text{m}}\text{Tc}$  half-life is 6.0 h and the photon energy is 140 keV (12).

In order to successfully use a radionuclide to image a GRF using gamma scintigraphy, the radionuclide needs to be retained by the GRF for an extended period of time. This can pose a serious challenge depending on the properties of the radionuclide within the gastric environment and the characteristics of the GRF. One common method to overcome the challenges of retention within a formulation is adsorption of the radionuclide onto an ion-exchange resin or activated charcoal prior to incorporation into the formulation. While this common radiolabeling approach has been used successfully for a variety of simple, oral formulations, GRFs provide additional challenges. By design, the GRFs are retained for an extended period of time in a low, yet fluctuating pH environment and subjected to compressive, mechanical digestive forces. Premature leakage of the radiolabel from the formulation may incorrectly suggest gastric emptying or disintegration of the GRF. In addition, if the approach of gastric retention based on a large size is pursued and a formulation is often required to swell 15 or more times its original size. The porosity of the final swollen formulation may be quite high, posing further challenges for retention of the radiolabel.

In this work, a large, swelling gastric retentive formulation was chosen as a model formulation. This formulation was shown to be difficult to radiolabel by conventional techniques and a novel technique for entrapment of a radionuclide is presented, in order to overcome the radiolabeling challenges of the model formulation within the gastric environment.

## MATERIALS AND METHODS

### Materials

$^{111}\text{In}$  indium chloride and  $^{99\text{m}}\text{Tc}$  technetium tin colloid was obtained from Photon Imaging (Research Triangle Park,

NC) for *in vitro* and preclinical evaluation and for clinical evaluation these materials were obtained from the Radiopharmacy, Western Infirmary, Glasgow, UK. Activated charcoal, sodium acetate, sodium chloride, hydrochloric acid, xanthan gum, locust bean gum, polyethylene glycol 400, hydroxypropylmethylcellulose, Amberjet<sup>®</sup> resins, Amberlite<sup>®</sup> resins and  $^{152}\text{Sm}$  samarium oxide were purchased from Sigma (St. Louis, MO). Cellulose acetate (CA-398) was obtained from Eastman (Kingsport, TN), Surelease<sup>®</sup> E-7-19010 was obtained from Colorcon (West Point, PA), Aquacoat<sup>®</sup> was obtained from FMC BioPolymer (Philadelphia, PA) and sugar spheres (30–35 mesh) were obtained from JRS Pharma (Patterson, NY).

### Gastro Retentive Formulation Manufacture

One gram of xanthan gum and 1 g of locust bean gum were dissolved in 100 ml of water using high shear mixing and heat. After dissolution of the polysaccharides, polyethylene glycol 400 was added to the solution and subsequently the radiolabel was added. The aqueous mixture was then poured into appropriate size molds and allowed to gel through the formation of physical crosslinks. After gelation, the formulation was placed in an Isotemp vacuum oven Model 282A with ThermoSavant RVT400 refrigerated vapor trap at 50°C to remove approximately 95% of the water. The dried gels were compressed, rolled and placed in a capsule (size 000). A more detailed description of this procedure can be found in Ayres (13).

### Dissolution Screening

The initial radioactivity of the radiolabeled GRF was measured in a Capintec Radioisotope Calibrator<sup>®</sup> Model CRC-12 and then placed in 500 ml of either pH 1.5 or pH 4.5 buffers in a Vankel USP II apparatus, with a stirring rate of 30 rpm and a temperature of 37°C. The radioactivity of the GRF was measured at either 30 min or 1 h intervals up to the 4 h followed by measurements at 8, 10 and 24 h. When the pH was fluctuated, the GRF was physically moved from one dissolution vessel at pH 1.5 to a second vessel at pH 4.5. The higher pH buffer was prepared by adding sodium acetate to a concentration of 25 mM and adjusting the pH to pH 4.5 with 1 M HCL. The low pH buffer was a 0.03 N HCL solution with 2% NaCl. No gastric enzymes were used in either dissolution media preparation.

### Scanning Electron Microscopy

The milled radiolabel particles were coated with a layer of gold (~10 nm) and observed with a Zeiss DSM-960 scanning electron microscope (Thornwood, NY) at a voltage of 15 kV.

### Samarium Oxide Bead Manufacture

Sugar spheres (30–35 mesh) were coated in a Glatt GPCG-1.1 (Ramsey, NJ) equipped with a 3.5 in diameter wurster column to a 13% weight gain of a 1:1 samarium oxide/hydroxypropylmethylcellulose mixture followed by a 15% weight gain barrier coat of ethylcellulose (Surelease<sup>®</sup>, Colorcon). The formulated samarium oxide beads were neutron irradiated at the Missouri

University Research Reactor facility prior to incorporation into the GRF.

### Absorption of Radionuclide onto Activated Charcoal or Ion Exchange Resins

One hundred thirty-one micro curie of  $^{111}\text{In}$  indium chloride in solution was added to a vial and filtered water was added until the volume reached 1 ml to dilute the indium. Fifty grams of ion exchange resin or activated charcoal were added to the solution and vortexed for 5 s. The mixture was dried in a vacuum oven at  $50^\circ\text{C}$  for 1 h. The dried powder was collected and incorporated into the GRF as stated above.

### Cellulose Acetate Radiolabel

After absorbing the radionuclide onto activated charcoal, the radiolabeled charcoal was combined with cellulose acetate in a 1:6 ratio and placed in an appropriate container for heating. The dry mixture was blended with a spatula to ensure uniformity, placed in a furnace or on a hot plate at an appropriate heat setting until the mixture was melted. The melted mixture was removed from heat and was allowed to cool to a brittle, glasslike consistency. Finally, the cooled, brittle mixture was transferred to a mortar for manual milling with a pestle.

### Theoretical Decay

The radioactive decay law was used to calculate the theoretical decay of the radioisotopes used,  $-\frac{dN}{dt} = \lambda N$  where  $N$  is the number of atoms remaining after decay time ( $t$ ) and  $\lambda$  is the decay constant. The half-life is related to the decay constant by the equation,  $T_{1/2} = \frac{0.693}{\lambda}$ . Also, the rate of decay of a radionuclide is described by its activity ( $A$ ), therefore,  $A = \lambda N$ . Combining these equations and integrating yields the following equation which was used to calculate the theoretical decay,  $A = A_0 e^{-\left(\frac{0.693t}{T_{1/2}}\right)}$ , where  $A$  indicates the activity,  $A_0$  is the initial activity,  $T_{1/2}$  is the half-life and  $t$  is the decay time.

### Effective Half-Life

The effective half-life was calculated by first modeling the dissolution data, specifically the release of the radiolabel from the GRF versus time, using the curve fitting function in Sigmaplot 9.0 (Point Richmond, CA). The equation used to model the data was,  $y = y_0 + ae^{-bx}$ , where  $y$  was the remaining activity in the GRF,  $x$  was the time and  $y_0$ ,  $a$  and  $b$  were outputs of the curve fitting function. The effective half-life,  $T_{1/2\text{eff}}$ , was calculated by dividing 0.693 by  $b$ . The equation used to model the data rewritten with the variables used in the theoretical decay equation in the preceding section became:  $A = C + A_0 e^{-\left(\frac{0.693t}{T_{1/2}}\right)}$ , where  $A$  indicates the activity,  $A_0$  is the initial activity,  $T_{1/2}$  is the half-life,  $t$  is the decay time,  $C$  is a constant and is an output of the curve fitting function. Typical,  $R^2$  values obtained from these curve fittings were 0.99. The batch to batch variability of effective half-life values was  $\pm 10\%$  or less. A simple exponential decay

function was not utilized because the dissolution vessel is a closed system. With a closed system, the radiolabel which has been released from the GRF is not removed and accumulates in the dissolution media. If the radiolabel concentration is high enough in the dissolution media, it will retard the release of the remaining radiolabel in the dissolution media.

### Preclinical Assessment of Radiolabel Performance

Two male mongrel dogs, similar in weight (17 kg), were housed in individual cages and received a standard diet (Canine food 5006, LabDiet<sup>®</sup>, IA, U.S.A.) and water ad libitum. The animals were clinically healthy and haematologically and biochemically normal throughout the experimental period. The research adhered to the "Principles of Laboratory Animal Care" (NIH publication #85-23, revised in 1985). Under an approved animal protocol adhering to humane treatment and principles of laboratory animal care, conscious mongrel dogs were comfortably seated in a sling, and situated beneath a gamma scintillation camera with the camera head located over the back of the mongrel. An E.C-am Fixed 180 dual head SPECT gamma camera (Siemens Medical Solutions, PA, U.S.A.) was equipped with two detectors, each having a  $533 \times 387$  mm field of view, fitted with low energy parallel hole collimators, and set for dual isotope acquisition where the pulse analyzer was tuned to 247 keV gamma ray of  $^{111}\text{In}$  (15% window) and 140 keV gamma ray of  $^{99\text{m}}\text{Tc}$  (8% window). The  $^{111}\text{In}$  labeled GRF was co-dosed with a  $^{99\text{m}}\text{Tc}$  labeled solid food to provide an outline of the stomach. One fiducial (reference marker) labeled with  $^{111}\text{In}$  was placed on each dog for proper positioning when placing the dog under the camera for image acquisition. Scintigraphic images of 30 s duration were simultaneously acquired from both anterior and posterior detectors at 1 h intervals up to 12 h and a final image was collected at 24 h. Between image acquisitions, the dogs were allowed to move freely in the room or were brought back to their cages. An on-line computer was connected to the camera and digital image recording was performed using an E.Soft programme (Siemens Medical Solutions).

### Clinical Assessment of Radiolabel Performance

This was a single-center, open-label, randomized cross-over study in six healthy male volunteers. The study followed the tenets of the Declaration of Helsinki in 1964 and its subsequent revisions, was approved by the North Glasgow Hospitals University Trust Ethics Committee and the Administration of Radioactive Substances Advisory Committee and was conducted to Good Clinical Practice. Six healthy male volunteers (age range 35–45 years, inclusive) with a body weight greater than 67 kg and a body mass index (BMI) within the range of 23.5–28.0  $\text{kg}/\text{m}^2$  participated in the study after providing written informed consent. All volunteers were non-smokers, were not taking any medication, had no abnormality on clinical examination, clinical chemistry or hematology examination, and no history of gastrointestinal disease. Subjects attended the study center on the evening prior to dosing and were given a standard evening meal ( $\sim 1,000$  kCal). One hour prior to dosing the subjects were given 100 ml of water. External radioactive

markers were taped to the anterior and lateral abdomen to allow accurate alignment of sequential images. Fifteen minutes prior to dosing each subject received a radiolabelled meal which consisted of one scrambled egg (labeled with 2 MBq of  $^{99m}\text{Tc}$ ), one piece of lightly buttered toast, and one cup of decaffeinated tea or coffee. The caloric value of the meal was  $\sim 280$  kCal. The meal was consumed within 15 min. Immediately after completion of the meal, the formulation was given with 240 ml of water. Subjects received a standard lunch ( $\sim 1,000$  kCal) at 5 h post dose, a standard snack ( $\sim 150$  kCal) at 7 h post dose, a standard evening meal ( $\sim 1,000$  kCal) at 10 h post dose, a standard snack ( $\sim 150$  kCal) at 13 h post dose and breakfast ( $\sim 280$  kCal) at 24 h post dose. Scintigraphic imaging was performed with the subject in a standing position, using a Siemens E.Cam SPECT gamma camera. Anterior and left lateral static acquisitions of 30 s duration were collected immediately after dosing, then every 30 min until 14 h post dose. Subsequent images were taken at 18 and 24 h post dose. Images were analyzed using the Weblink image analysis program. For each subject, an image that presented a full, clearly defined stomach shape was selected, and regions of interest (ROI) were drawn around the stomach shape and anatomic marker. A further ROI was drawn in the field of view in order to account for background radiation levels. The counts per cell within each ROI were then determined. The same ROIs were used to analyze each image in the data set. The external radioactive marker was used to align the ROIs in each image. All data were then corrected for radioactive decay, background and expressed in terms of corrected counts per cell within each ROI. Two independent trained operators separately assessed each scintigraphic image. Gastric emptying time of the formulation was determined as well as gastrointestinal transit. All formulations were manufactured in accordance with Good Manufacturing Practices (GMP) as required by the ICH Guidelines for Good Clinical Practice (GCP).

## RESULTS AND DISCUSSION

### *In vitro* Radiolabel Retention Evaluations

*In vitro* dissolution is a common technique used to characterize the release of a drug substance from a pharma-

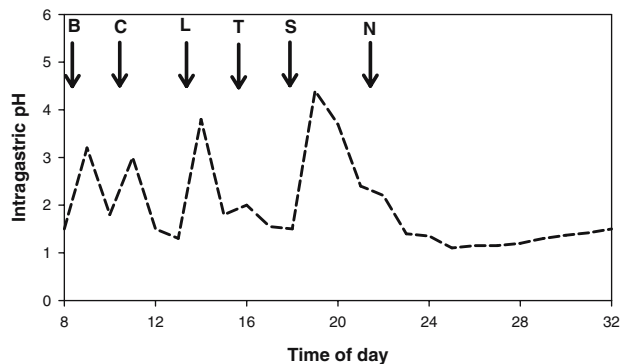


**Fig. 1.** Data shown are median intragastric pH data from 23 healthy subjects. Letters indicate beginning of each meal, B Breakfast, C coffee, L lunch, T tea, S supper, N nighttime snack. Reproduced with permission (15).

ceutical formulation and is also an effective tool to determine if a radionuclide is successfully retained in a formulation for the amount of time required. The most common pH used to mimic the gastric environment is pH 1.0 or 1.5 for the fasted stomach pH, however, during the fed state the average gastric pH is pH 4.5 (14). Therefore, the retention of the radionuclide in the GRF was evaluated at both pH 1.5 and pH 4.5. However, as shown in Fig. 1, the gastric pH fluctuates widely over time (15). This is a critical factor to consider especially when testing a GRF formulation, which will reside for long time in the stomach environment and can be sensitive to pH. When an effective radiolabel was identified, a subsequent *in vitro* dissolution evaluation was performed to determine the effect of gastric pH fluctuations. The GRFs were exposed to the following pH fluctuations: pH 4.5 for 2 h, pH 1.5 for 6 h, pH 4.5 for 2 h and pH 1.5 for 14 h, and the retention of the radiolabel in the GRF was evaluated during each stage.

### Samarium Oxide

$^{153}\text{Samarium}$ ,  $^{111}\text{indium}$  and  $^{99m}\text{technetium}$  all represent ideal radionuclide candidates for gamma scintigraphy evaluations. However, because of the substantial time span ( $\sim 24$  h) required for manufacturing the GRF used in this study,  $^{99m}\text{Tc}$  was not utilized due the short half-life compared to  $^{111}\text{In}$  and  $^{153}\text{Sm}$ .  $^{153}\text{Samarium}$  oxide was the first radiolabel evaluated for the GRF. Additionally,  $^{152}\text{samarium}$  oxide ( $\text{Sm}_2\text{O}_3$ ) allows manufacture of the GRF using a non-radioactive form of  $^{152}\text{samarium}$  which will then be neutron irradiated alone or in the final dosage form. However, if the neutron irradiation route is chosen, the impact of the nuclear reactor core exposure on the dosage form should be evaluated. For this study, the  $^{152}\text{samarium}$  oxide ( $\text{Sm}_2\text{O}_3$ ) powder was neutron irradiated to form the radioactive  $^{153}\text{samarium}$  oxide ( $\text{Sm}_2\text{O}_3$ ) powder prior to incorporation into the GRF in order to avoid exposure of the GRF to the nuclear reactor core. Figure 2a and b present the results of the dissolution of the GRF manufactured with  $^{153}\text{samarium}$  oxide powder. The theoretical profiles in Fig. 2a and b represent the ideal case, where loss of radioactivity is solely due to radioactive decay. The measured profiles in Fig. 2a and b reveal that the  $^{153}\text{samarium}$  oxide was rapidly released at a pH of 1.5, while at pH 4.5, the radionuclide was retained up to 90 min with minimal to no leakage followed by a more significant release after 90 min but still at a significantly slower rate than the pH 1.5 condition. The performance of  $^{153}\text{samarium}$  oxide powder at pH 1.5 or pH 4.5 was judged to be inadequate to radiolabel the GRF. One explanation for the difference observed in the performance of the radiolabel at pH 1.5 versus pH 4.5 can be offered by the functional groups on the polysaccharides, locust bean gum and xanthan gum, used to manufacture the GRF. Locust bean gum is composed of mannose and galactose sugar units which are not ionized at the pHs studied, however, xanthan gum is a heteropolysaccharide composed of glucose, mannose and glucuronic acid as well as acetyl and pyruvate substituents (16). The pKa of carboxylic acid functional groups on xanthan gum has been reported to be in the range of 2.6–2.8 (17). Therefore, at pH 4.5 the carboxylic acid groups of xanthan gum would be ionized and may create electro-

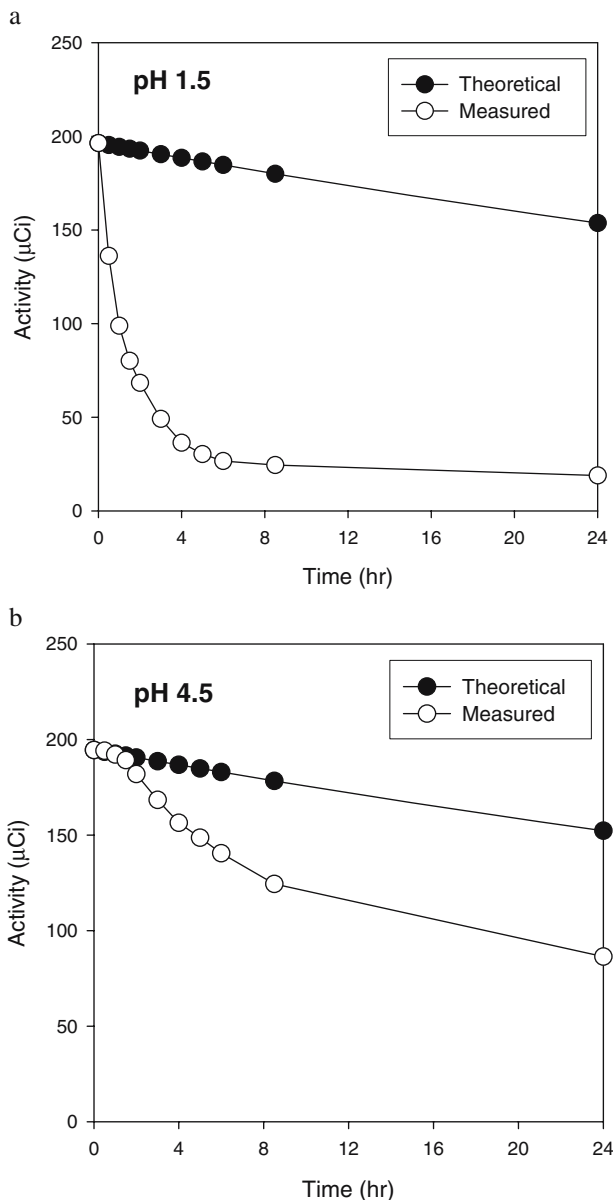


**Fig. 2.** a Dissolution at pH 1.5 of a GRF with <sup>153</sup>Samarium Oxide powder. b Dissolution at pH 4.5 of a GRF with <sup>153</sup>Samarium Oxide powder. The theoretical profiles represent the ideal case, where loss of radioactivity is solely due to radioactive decay. The measured profiles are the radioactivity value of the GRF at each timepoint.

static interactions with the <sup>153</sup>samarium oxide, reducing its diffusion out of the GRF. At pH 1.5, the carboxylic acid groups of xanthan gum are protonated and the same electrostatic interactions would not occur. Essentially, the GRF would not be ionized and the samarium would be free to diffuse out of the GRF. Diffusion studies using laser confocal scanning microscopy of similar crosslinked polysaccharides has shown that the diffusion coefficient inside these hydrogels does not vary substantially from the diffusion coefficient in water until very high crosslinking levels are obtained (18). Based on this information, the lack of ionized carboxylic acids and the high diffusion coefficient in typical polysaccharide hydrogels could explain the rapid release of the radiolabel at pH 1.5.

**Effective Half-Life**

During evaluation of the GRF with samarium oxide powder it was observed that the rate of radiolabel release from the GRF occurred in a similar fashion to an exponential decay process. This is consistent with Fick’s second law of diffusion which states that the change in concentration with time in a particular region is proportional to the change in the concentration gradient at that point in the system (19). This represents a first order process which can be modeled by an exponential function in the ideal case. Therefore, by modeling the radiolabel release from the GRF with an exponential function, we obtain an effective half-life activity-time profile for the radiolabel in the GRF as shown in Fig. 3 ( $T_{eff1/2}$  model). The initial exponential equation utilized was:  $A = A_0 e^{-\left(\frac{0.693}{T_{1/2eff}} t\right)}$ , where  $A$  indicates the activity,  $A_0$  is the initial activity,  $T_{1/2eff}$  is the effective half-life and  $t$  is the decay time. However, a simple exponential fit did not appropriately describe the measured radiolabel release at the later timepoints. In this experiment, the dissolution vessel has a fixed volume of media; therefore, as more radiolabel was released into the media, an artificial decrease in the concentration gradient was created impacting radiolabel diffusion. This reduced the release of the radiolabel out of the GRF. To account for this, a constant,  $C$ , was added to the equation,  $A = C + A_0 e^{-\left(\frac{0.693}{T_{1/2eff}} t\right)}$ , in order to account for the reduced concentration gradient and lack of sink conditions at the later timepoints. Using this improved model, radiolabel performance can be correctly quantified and different radiolabel formulations can be easily compared. If the radiolabel was truly entrapped in the GRF, the radioactivity decrease would be similar to the radioactive decay of the radionuclide; however, if the radiolabel was diffusing out of

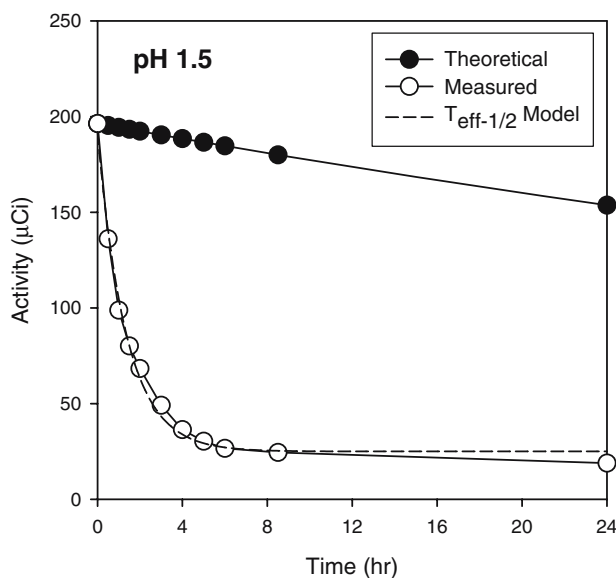


**Fig. 3.** Dissolution at pH 1.5 of a GRF with <sup>153</sup>Samarium Oxide powder versus exponential decay modeling of the  $T_{1/2eff}$  effective half life using the exponential decay model,  $A = C + A_0 e^{-\left(\frac{0.693}{T_{1/2eff}} t\right)}$ , where  $A$  indicates the activity,  $A_0$  is the initial activity,  $T_{1/2eff}$  is the effective half-life,  $t$  is the decay time and  $C$  is a constant calculated during curve fitting.

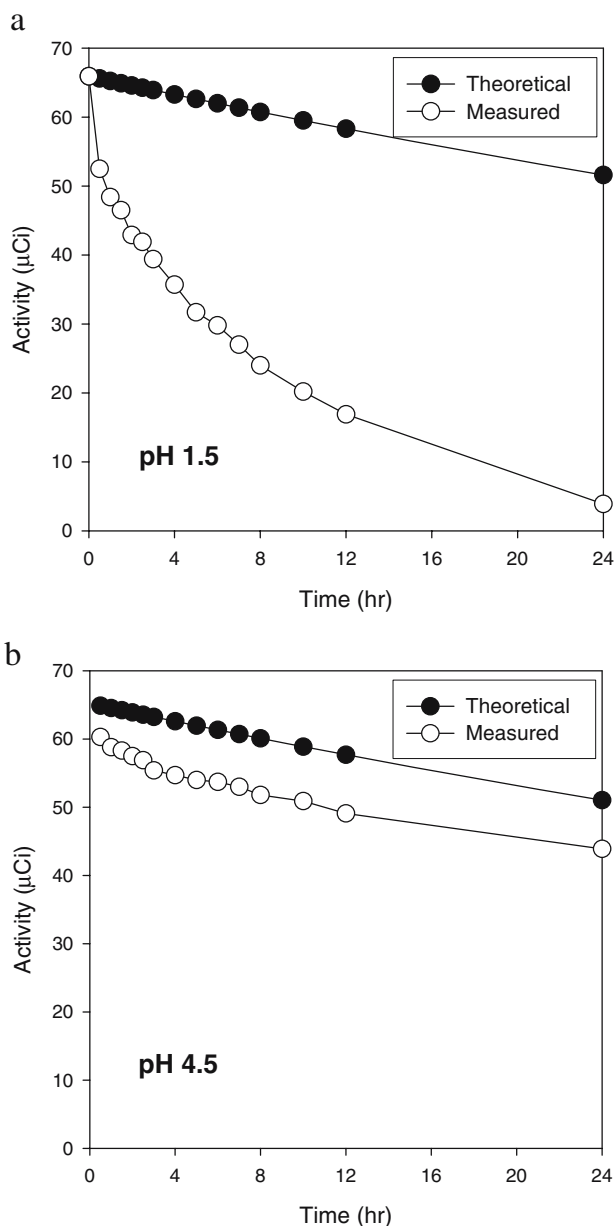


**Fig. 4.** a Dissolution at pH 1.5 of a GRF with  $^{111}\text{In}$  Chloride powder. b Dissolution at pH 4.5 of a GRF with  $^{111}\text{In}$  Chloride powder.

the GRF, the decrease in radioactivity of the GRF would result in a decreased  $T_{1/2\text{eff}}$ . Therefore, based on the effective half-life, we were able to estimate if the radiolabel concentration in the GRF was sufficient to allow the GRF to be imaged up to 24 h using gamma scintigraphy. To allow this, at a minimum, a  $T_{1/2\text{eff}}$  in both pH 1.5 and 4.5 should have been higher than 10 h. The calculated  $T_{1/2\text{eff}}$  for  $^{153}\text{Sm}$  powder was 0.9 and 5.2 h, at pH 1.5 and 4.5, respectively. Based on this data, the performance of  $^{153}\text{Sm}$  powder was judged to be inadequate to radiolabel the GRF.

Developing a radiolabeled GRF with a satisfactory  $T_{1/2\text{eff}}$  was important not only for accurate assessment of GRF performance, but also for safety reasons. In exploratory clinical studies with GRFs, it is vital to ensure that the GRF has emptied from the stomach and endoscopic proce-

dures are not needed to investigate the location and potentially remove the GRF.

### Samarium Oxide Beads

Simple addition of  $^{153}\text{Sm}$  samarium oxide incorporated directly to the GRF during the manufacturing process did not provide a robust radiolabeling method; therefore, neutron irradiated,  $^{153}\text{Sm}$  samarium oxide coated beads with an outer layer of insoluble ethylcellulose to further entrap the radiolabel were evaluated. The beads were incorporated into the GRF during manufacture in a similar fashion as the  $^{153}\text{Sm}$  samarium oxide powder. The results were improved compared to  $^{153}\text{Sm}$  samarium oxide powder with a calculated  $T_{1/2\text{eff}}$  of 3.9 and 9.8 h, at pH 1.5 and 4.5, respectively; however, it did not reach the targeted  $T_{1/2\text{eff}}$  of  $\sim 10$  h at pH 1.5. In addition, the large size of the coated beads (600–700  $\mu\text{m}$ ) reduced the gel strength of the GRF by approximately 50%, since a weaker gel is expected to brake down quickly due to the stomach digestive contractions, this effect could have compromised gastric retentive performance of the formulation.

### Indium Chloride

As an alternative to  $^{153}\text{Sm}$  samarium oxide,  $^{111}\text{In}$  indium chloride was also screened for radiolabel performance in the GRF because of its ideal half-life and photon energy.  $^{111}\text{In}$  indium chloride was added to the GRF during manufacture in a similar fashion to the  $^{153}\text{Sm}$  samarium oxide. Figure 4 displays the theoretical and measured radioactivity loss with time for the GRF in both pH 1.5 and pH 4.5. The theoretical profiles in Fig. 4a and b represent the ideal case, where loss of radioactivity is solely due to radioactive decay. Since  $^{111}\text{In}$  indium chloride like  $^{153}\text{Sm}$  samarium oxide is an electrovalent bond, it is a weak bond that readily dissociates. Consistent with  $^{153}\text{Sm}$ , there was significant leakage of the  $^{111}\text{In}$  at pH 1.5. However, at pH 4.5 the radiolabel retention was substantial. The calculated  $T_{1/2\text{eff}}$  is shown for both pHs in Table I. During the first 30 min, there was a rapid loss of radiolabel of approximately 10–20%; however, after that initial radioactivity loss, the performance mimicked the predicted radioactivity decay. Most likely this behavior was due to complexation of the  $^{111}\text{In}$  with ionized carboxylic acid groups of the xanthan gum at pH 4.5. Additionally, as an alternative explanation, below pH 3 indium exists in a soluble, ionic form as the hexaaqua complex  $[\text{In}(\text{H}_2\text{O})_6]^{3+}$ , while above pH 3, this metal forms an insoluble hydroxide,  $\text{In}(\text{OH})_3$ , which could be entrapped in the GRF (12). Regardless of the mechanism, the  $^{111}\text{In}$  radiolabel retention

**Table I.** Effective Half-life: Indium Chloride Based Radiolabels in a Gastric Retentive Formulation

	pH 1.5 (h)	pH 4.5 (h)
$^{111}\text{InCl}_2$ Powder	5.3	10.2
$^{111}\text{InCl}_2$ —Amberjet	4.1	25.7
$^{111}\text{InCl}_2$ —Activated Charcoal (AC)	1.5	2.9
$^{111}\text{InCl}_2$ —AC-Cellulose Acetate	11.4	42

$^{111}\text{InCl}_2$  half life is 67.2 h

**Table II.** Summary of Radiolabeling Procedure via Polymer Melt Entrapment

Step #	Instructions
1	Add the $^{111}\text{InCl}_2$ to the activated charcoal.
2	To ensure uniform absorption of the radiolabel on the charcoal, add an appropriate amount of water or weak acid sufficient to wet the activated charcoal.
3	Dry the activated charcoal.
4	Combine the dried, radiolabeled charcoal with cellulose acetate (1:6) and blend the mixture.
5	Heat mixture until molten
6	Allow mixture to cool.
7	Using a spatula, break the brittle mixture into smaller pieces and transfer into a mortar for milling with pestle.
8	Once the milled mixture has consistent particle size it is ready to be incorporated into the GRF.

at pH 4.5 was highly successful, yet when considering both pHs, the radiolabel was insufficient for extended gastric imaging of the GRF in clinical studies.

#### Indium Chloride Absorbed to Activated Charcoal or Ion Exchange Resins

A common technique for developing a more robust radiolabel is to adsorb the radionuclide onto an ion exchange resin or other medium such as activated charcoal, prior to incorporation into the dosage form (20). A series of ion exchange resins were investigated, but with poor results. Amberjet 4400 was the ion exchange resin which had the best performance in retaining the radiolabel in the GRF. Amberjet 4400 provided exceptional protection at pH 4.5, however, at pH 1.5 it actually decreased radiolabel retention compared to  $^{111}\text{indium}$  chloride alone (Table I). Adsorption of  $^{111}\text{indium}$  chloride onto activated charcoal was also evaluated but radiolabel performance was significantly decreased pHs compared to simple indium chloride addition at both pHs (Table I). The reasons for this are unclear.

#### Indium Chloride Polymer Encapsulation

Due to the lack of success with the methods described above, the radionuclide was coated with an insoluble polymer to reduce radiolabel loss from the GRF. This was performed to provide a protective layer in order to reduce radiolabel leakage, and also to generate a smaller radiolabeled particle compared to the radiolabeled beads described above which reduced the gel strength of the GRF. In order to avoid using polymers in solution, which could cause segregation of the radiolabel and polymer during evaporation of the solvent, a polymer melt approach was attempted. Cellulose acetate was the polymer selected for this evaluation. The  $^{111}\text{indium}$  chloride was first absorbed onto activated charcoal, and then dry blended with cellulose acetate in a ratio of one part  $^{111}\text{indium}$  chloride/activated charcoal to six parts cellulose acetate. The  $^{111}\text{indium}$  chloride was supplied as a solution, so adsorption onto activated charcoal improved handling of the dried powder and improved dry blend uniformity. The dry

blend was placed in a suitable glass container on a hot plate until the mixture became molten. The melted mixture was cooled to room temperature to form a brittle glass that could be ground to a particle size of less than  $50\ \mu\text{m}$  using a mortar and pestle. These milled particles will be referred to as polymer encapsulated  $^{111}\text{indium}$  chloride (PEIC). A summary of the method is shown in Table II.

Scanning electron microscopy (SEM) was performed to gain greater insight into the morphology of the PEIC (Fig. 5a and b). The SEM images revealed that the majority of the milled particles were between  $5\text{--}20\ \mu\text{m}$  and had a smooth, glassy surface; however, smaller particles (less than  $1\ \mu\text{m}$ ) were also present. These smaller particles may preferentially

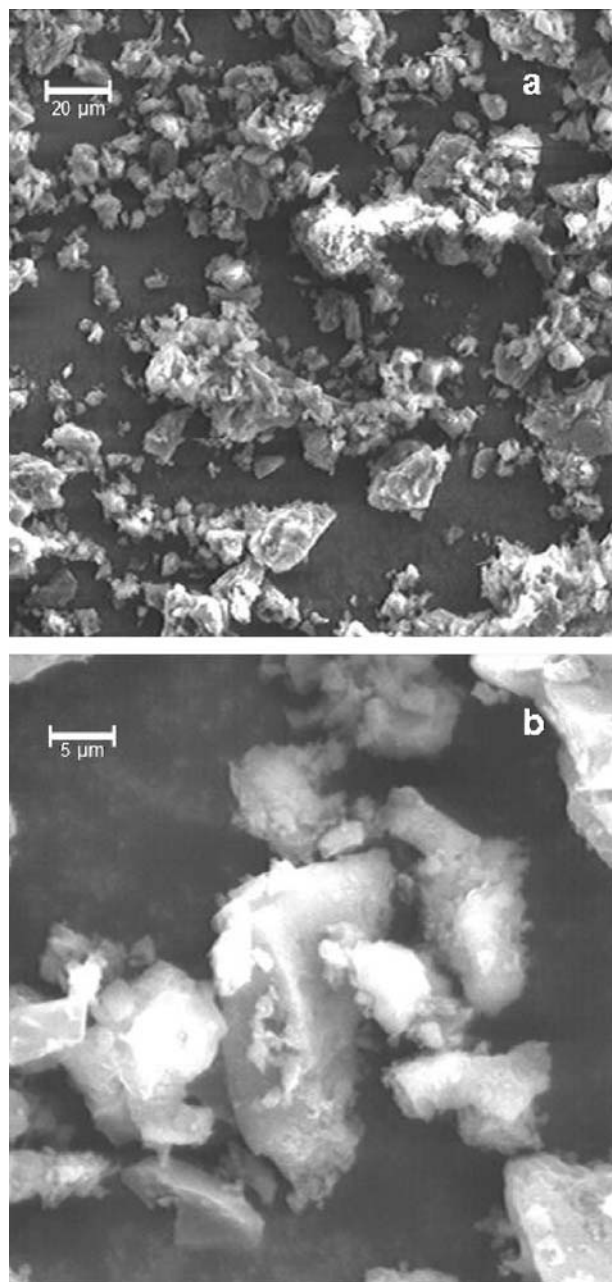


**Fig. 5.** Scanning electron microscopy was performed on the PEIC radiolabel at a  $\times 500$  magnification and b  $\times 3,000$  magnification of a particle with rougher texture.

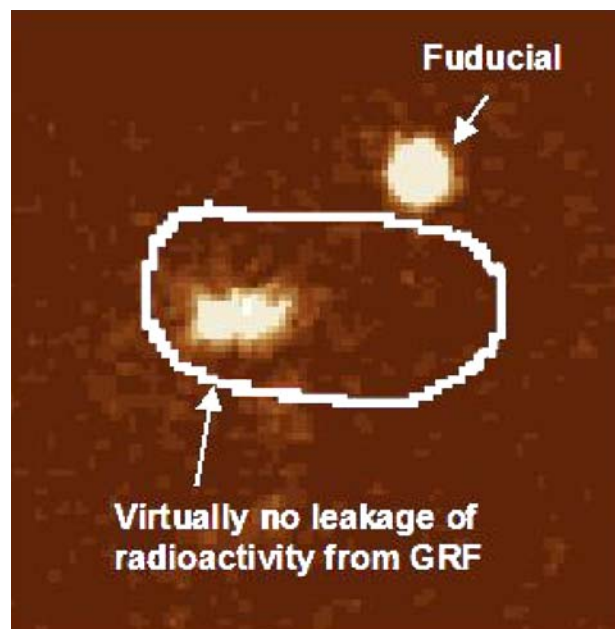
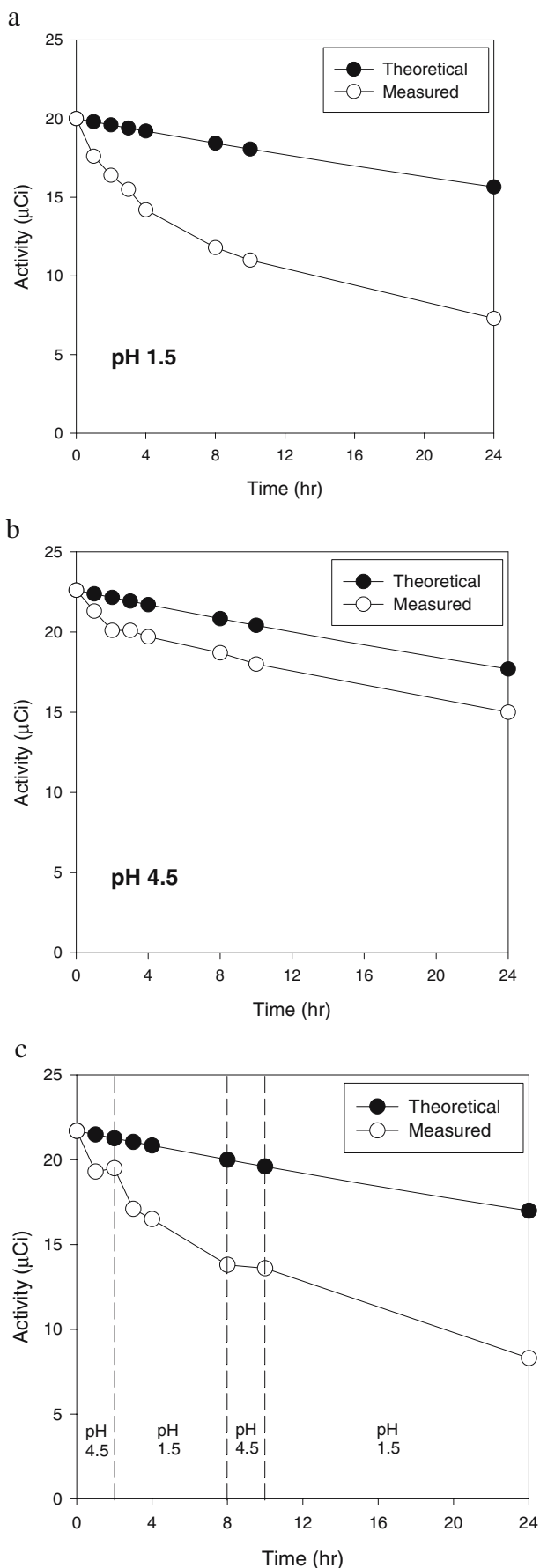


**Fig. 7.** PEIC radiolabeled GRF in the stomach of a mongrel dog, 11 h post-dose. Virtually no leakage of the radiolabel was observed. The stomach outline is based on imaging a co-dosed  $^{99\text{m}}\text{Tc}$  Technetium labeled solid food.

leak out of the GRF, while the larger particles would be retained within the GRF if leakage of the radiolabel is solely due to the size of the milled particles relative to the “pores” of the intertwined polymers of the GRF. A possible process improvement would be sieve screening of the milled particles in order to remove the fines; however this process was not performed in this work to reduce the complexity of the approach and the radioactive contamination of equipment.

Dissolution screening of GRFs radiolabeled with PEIC resulted in the least leakage of the radiolabel in pH 1.5 media compared to previous attempts (Table I). Low pH was consistently the most difficult media in which to retain the radiolabel within the GRF and the  $T_{1/2\text{eff}}$  for the PEIC at pH 1.5 was 11.4 h. As previously observed with other methods, the radiolabel integrity in pH 4.5 buffer was excellent and closely matched the radioactivity decay of the radionuclide. The radiolabel retention was also acceptable when the media pH was fluctuated between 1.5 and 4.5, simulating the intraday gastric pH fluctuations (Fig. 6). The results from the PEIC were substantially better than the previously attempted radiolabels and therefore, it was progressed for an *in vivo* pre-clinical evaluation.

While cellulose acetate was selected as the polymer of choice in this work, it may be possible to use the same procedure with alternative polymers such as ethylcellulose. Polymers used for enteric coating may also be considered, however several reasons supported the use of an insoluble polymer. In the pre-clinical studies, we employed dogs as the species of choice and, based on in-house data, the pH of a canine stomach can be much higher than in humans leading

**Fig. 6.** a Dissolution at pH 1.5 of a GRF with the PEIC radiolabel. b Dissolution at pH 4.5 of a GRF with the PEIC radiolabel. c Dissolution at alternating pH 1.5 and 4.5 of a GRF with the PEIC radiolabel.

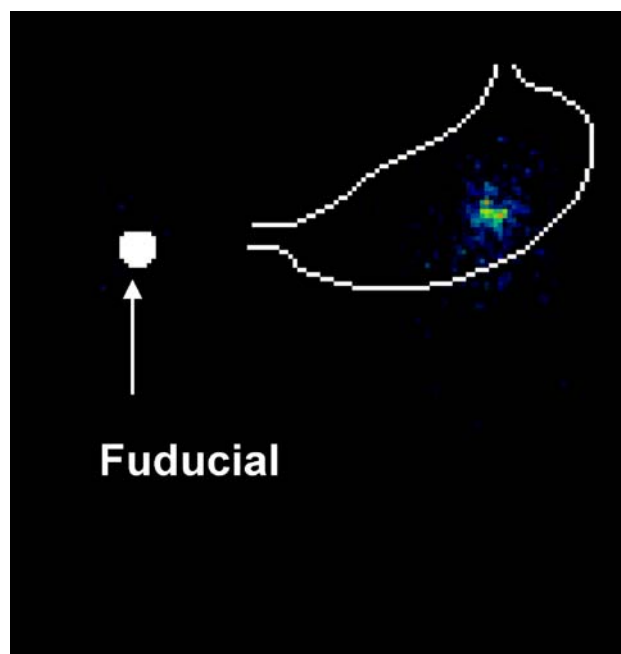


**Fig. 8.** PEIC radiolabeled GRF in the stomach of healthy human volunteer, 18 h post dose. Virtually no leakage of the radiolabel was observed. The stomach outline is based on imaging a co-dosed  $^{99m}\text{Tc}$  labeled egg.

to false negatives for retention of the radiolabel when using enteric polymers. In addition, it is possible that subjects recruited for the clinical studies had an unusually high pH, and, since we did not measure gastric pH, this would have created a false negative result as well. Finally, while this was not the focus of the paper, an insoluble polymer also allowed gastrointestinal transit estimation after gastric emptying, visualization if the GRF degraded/broke down in the lower intestines and verification that the GRF did not cause an intestinal occlusion in the event that it emptied from the stomach prematurely.

### **In vivo Evaluation**

Based on a series of publications evaluating gastric retentive formulations comprising non-disintegrating geometric shapes *in vitro* and *in vivo*, it was decided to evaluate the radiolabeled GRF in a large dog model due to an improved correlation to man compared to smaller dog models (2,21,22). In the cited studies, the beagle dog (10–15 kg) retained the GRF for a substantial period of time, while the performance when tested in man was significantly shorter. This prompted the authors to evaluate a larger dog model, the foxhound (30–40 kg) which continued to result in prolonged retention compared to the performance in man, yet it was more predictive than the beagle dog. For our studies, the foxhound dog model was not available, but an intermediate size mongrel dog model (15–20 kg) was available and used for evaluation of the PEIC radiolabel in the GRF. Dosing of the GRF in mongrel dogs revealed virtually no leakage of the radiolabel even after 11 h post dose as shown in Fig. 7. This result revealed that the *in vivo*

complexity of gastric environment, including digestive, compressive forces on the GRF, did not cause premature release of the radiolabel. This further strengthened our confidence in the *in vitro* results, and suggested that the PEIC radiolabel retention was excellent.

Based on the successful *in vitro* and pre-clinical radiolabel retention, the PEIC radiolabeled GRF was progressed to an exploratory clinical study. Figure 8 shows an 18 h image of a healthy subject with the PEIC radiolabeled GRF still retained in the stomach and clearly visible with gamma scintigraphy. In fact, the location of the GRF could be determined by scintigraphic assessment even beyond 48 h and allowed complete GI transit time estimation.

The PEIC radiolabeling technique described here continued to be used successfully in two clinical gamma scintigraphy studies with a total of 63 doses administered. The results of these clinical studies are beyond the scope of this manuscript and will be reported elsewhere. This successful radiolabeling technique will continue to be applied to study future GRFs; furthermore, based on the ability of this radiolabel to generate complete GI transit time information, the same approach would be useful for studying the transit of more traditional dosage forms as well. Finally, pharmacoscintigraphic studies could also be performed with the PEIC radiolabel GRFs. The location of the dosage form within the GI tract and the pharmacokinetic concentration-time profiles for the compound of interest could be correlated using this technique. This would allow insight into the absorption of the drug in various regions of the GI tract and definitely determine if a gastric retentive dosage form would generate a successful PK/PD performance.

### **CONCLUSION**

A novel method of polymer encapsulation has been developed to substantially retard the release of a radionuclide from a GRF in acidic pH environments. The radiolabel retention is critically important for gastric retentive formulations, which, by design, are exposed to a fluctuating low pH environment for prolonged periods of time. In this study, the mechanism of gastric retention was based on a large size, and thus the formulation swelled substantially generating a highly porous structure. This porous structure prematurely released typical radiolabels and required an enhanced radiolabel methodology for sufficient retention of the radionuclide. The method developed in this manuscript overcomes the challenges of radiolabel retention for GRFs and could be used as a standard radiolabel method to evaluate gastric retentive formulations using gamma scintigraphy.

### **REFERENCES**

1. E. A. Klausner, E. Lavy, M. Friedman, and A. Hoffman. Expandable gastroretentive dosage forms. *J. Control. Release* **90**:143–162 (2003).
2. J. A. Fix, R. Cargill, and K. Engle. Controlled gastric emptying. III. Gastric residence time of a nondisintegrating geometric shape in human volunteers. *Pharm. Res.* **10**(7):1087–1089 (1993).
3. E. A. Klausner, E. Lavy, M. Barta, E. Cserepes, M. Friedman, and A. Hoffman. Novel gastroretentive dosage forms: evaluation of gastroretentivity and its effect on levodopa absorption in humans. *Pharm. Res.* **20**(9):1466–1473 (2003).

4. F. Kedzierewicz, P. Thouvenot, J. Lemut, A. Etienne, M. Hoffman, and P. Maincent. Evaluation of peroral silicone dosage forms in humans by gamma-scintigraphy. *J. Control. Release* **58**:195–205 (1999).
5. W. Webb. Management of foreign bodies of the upper gastrointestinal tract: update. *Gastrointest. Endosc.* **41**:39 (1995).
6. H. Koch. Operative endoscopy. *Gastrointest. Endosc.* **24**(2):65 (1977).
7. H. Kato, M. Nakamura, E. Orito, R. Ueda, and M. Mizokami. The first report of successful nasogastric coca-cola lavage treatment for bitter persimmon phytobezoars in Japan. *Am. J. Gastroenterol.* **98**(7):1662–1663 (2003).
8. A. Steingoetter, D. Weishaupt, P. Kunz, K. Mader, H. Lengsfeld, M. Thurnshirn, P. Boesiger, M. Fried, and W. Schwizer. Magnetic resonance imaging for the *in-vivo* evaluation of gastric-retentive tablets. *Pharm. Res.* **20**(12):2001–2007 (2003).
9. Given Imaging (<http://www.givenimaging.com>)
10. W. Weitschies, R.-S. Wedemeyer, O. Kosch, K. Fach, S. Nagel, E. Söderlind, L. Trahms, B. Abrahamsson, and H. Mönnikes. Impact of the intragastric location of extended release tablets on food interactions. *J. Control. Release* **108**:375–385 (2005).
11. P. Goethals, A. Volkaert, B. Van Vlem, and R. Vanholder. Critical evaluation of the chemical standardization procedure for measuring gastric emptying of solids. *J. Label. Compd. Radiopharm.* **45**:1091–1096 (2002).
12. R. J. Kowalsky, and S. W. Falen. *Radiopharmaceuticals in Nuclear Pharmacy and Nuclear Medicine*, 2nd ed. American Pharmacists Association, Washington, DC, 2004.
13. J. W. Ayres. Expandable gastric retention device. US Patent Application #20040219186-A1, Nov. 4, 2004.
14. J. D. Gardner, A. A. Ciociola, and M. Robinson. Measurement of meal-stimulated gastric acid secretion by *in-vivo* gastric autotitration. *J. Appl. Physiol.* **92**:427–434 (2002).
15. M. P. Williams, J. Sercombe, M. I. Hamilton, and R. E. Pounder. A placebo-controlled trial to assess the effects of 8 days of dosing with rabeprazole versus omeprazole on 24-h intragastric acidity and plasma gastrin concentrations in young healthy male subjects. *Aliment. Pharmacol. Ther.* **12**:1079–1089 (1998).
16. V. Pai, M. Srinivasarao, and S. A. Khan. Evolution of microstructure and rheology in mixed polysaccharide systems. *Macromolecules* **35**:1699–1707 (2002).
17. S. J. J. Debon, and R. F. Tester. *In vitro* binding of calcium, iron and zinc by non-starch polysaccharides. *Food Chem.* **73**(4):401–410 (2001).
18. M. D. Burke, J. O. Park, M. Srinivasarao, and S. A. Khan. Diffusion of macromolecules in polymer solutions and gels: a laser scanning confocal microscopy study. *Macromolecules* **33**(20):7500–7507 (2000).
19. A. Martin. *Physical Pharmacy*, 4th ed. Lea and Febiger, Philadelphia, 1993.
20. A. Keshavarzian, W. E. Barnes, K. Bruninga, B. Nemchausky, H. Mermall, and D. Bushnell. Delayed colonic transit in spinal cord-injured patients measured by indium-111 Amberlite scintigraphy. *Am. J. Gastroenterol.* **90**:1295–1300 (1995).
21. R. Cargill, L. J. Caldwell, K. Engle, J. A. Fix, P. A. Porter, and C. R. Gardner. Controlled gastric emptying. I. Effects of physical properties on gastric residence times of nondisintegrating geometric shapes in beagle dogs. *Pharm. Res.* **5**:533–536 (1988).
22. R. Cargill, K. Engle, C. R. Gardner, and J. A. Fix. Controlled gastric emptying. II. *In vitro* erosion and gastric residence times of an erodible device in beagle dogs. *Pharm. Res.* **6**(6):506–509 (1989).